TOPICAL REVIEW — Iron-based high temperature superconductors

Spin, charge, and orbital orderings in iron-based superconductors*

Jiang Qing(江 庆), Kang Yao-Tai(康耀太), and Yao Dao-Xin(姚道新)†

State Key Laboratory of Optoelectronic Materials and Technology, School of Physics and Engineering, Sun Yat-Sen University, Guangzhou 510275, *China*

(Received 14 June 2013; revised manuscript received 23 June 2013)

In this article, we briefly review spin, charge, and orbital orderings in iron-based superconductors, as well as the multi-orbital models. The interplay of spin, charge, and orbital orderings is a key to understand the high temperature superconductivity. As an illustration, we use the two-orbital model to show the spin and charge orderings in iron-based superconductors based on the mean-field approximation in real space. The typical spin and charge orderings are shown by choosing appropriate parameters, which are in good agreement with experiments. We also show the effect of Fe vacancies, which can introduce the nematic phase and interesting magnetic ground states. The orbital ordering is also discussed in iron-based superconductors. It is found that disorder may play a role to produce the superconductivity.

Keywords: iron-based superconductors, multi-orbital models, magnetic ordering, charge stripe

PACS: 74.25.–q, 74.70.Xa, 74.20.–z, 74.25.Ha **DOI:** 10.1088/1674-1056/22/8/087402

1. Introduction

It has been five years since the discovery of superconductivity at 26 K in LaFeAsO doped with F in 2008,[1] great progresses have been made in the field of high temperature iron-based superconductivity. Many compounds of iron-based superconductors have been found and new materials are still being discovered. Basically, they can be divided into two categories, pnictides and chalcogenides. On the other hand, they can also be divided as 1111 compounds (e.g., LaFeAsO), 122 compounds (e.g., $SrFe_2As_2$), 111 compounds (e.g., LiFeAs), 11 compounds (e.g., FeTe/Se), 245 compounds (e.g., $K_2Fe_4Se_5$), and so on. All these materials share a common layered structure based on a planar layer of iron atoms joined by pnictogen or chalcogen anions. It is widely believed that their superconductivity is based on the common iron layers, similar to the cuprate superconductors. The modern experimental probes, such as angle-resolved photoemission spectroscopy (ARPES),[2,3] scanning tunneling microscopy (STM),[4–6] neutron scattering,[7–9] inelastic X-ray scattering (RIXS),[10,11] and X-ray diffraction (XRD),[12] can provide important information for these materials.

Most parent compounds of iron-based superconductors are bad metals (245 compounds are semiconductors), which is an important difference between iron-based and cuprate superconductors. Band structure calculations have shown a finite density of states near the Fermi level.[13] Fermi pockets and finite resistances are observed in ARPES experiments and transport experiments, respectively.[14–17] These results support the importance of itinerant electrons. On the other hand, local density approximation (LDA) band structure calculations indicate that the Fe 3d orbitals are strongly hybridized, and play a key role in the density of states near the Fermi level, especially d_{xz} and d_{yz}.[18,19] This character suggests that iron-based superconductors have a multi-orbital nature, which is different from cuprates.

Although the pairing symmetry is still under debate, it is apparently not the conventional s wave. Actually, an $s^{\pm}$ wave pairing symmetry is more favored,[18,20–22] and short range spin fluctuations are believed to be a medium for Cooper pairing. Before doping, the parent compounds of most iron-based superconductors show long range antiferromagnetic orders. From the local moment picture, the phase can be described by a J_1–J_2 type Heisenberg model.[23–27] The corresponding spin wave calculations can give consistent magnetic excitations with neutron scattering experiments.[7,28,29] The magnetism can also be understood by the itinerant electron picture because the parent compounds are bad metals. Within this picture, the long range magnetic order arises from the Fermi surface nesting. It is worth mentioning that iron-based superconductors may share a common mechanism with cuprates, though they have different pairing symmetries. An S_4 model proposed by Hu *et al.* recently showed that an $s^{\pm}$ wave pairing in iron-based superconductors can be connected to a d wave pairing.[30]

Before applying any effective theoretical models to iron-based superconductors, we need to know how strong the electron correlations are in these materials. The metallic nature tells us that the correlations are relatively weaker compared to cuprates whose parent compounds are Mott insulators. More

*Project supported by the National Basic Research Program of China (Grant No. 2012CB821400), the National Natural Science Foundation of China (Grant Nos. 11074310 and 11275279), the Specialized Research Fund for the Doctoral Program of Higher Education, China (Grant No. 20110171110026), and the Program for New Century Excellent Talents in University, China (Grant No. NCET-11-0547).

†Corresponding author. E-mail: yaodaoxin@gmail.com

© 2013 Chinese Physical Society and IOP Publishing Ltd

in-depth studies suggest that most iron-based superconductors are in the intermediately-correlated regime.[31,32] Because in most iron-based superconductors, the on-site Coulomb repulsion U is found in an intermediate range between the strong correlation side (cuprate superconductors) and the non-interacting side (BCS superconductors) based on the fact that most parent compounds of the iron-based superconductors are antiferromagnetic (AF) bad metals with poor conductivity.[33] Numerical calculations indicate that U for Fe in iron-based superconductors is approximately half of that for Cu in cuprates.[34]

Actually, it is not completely right to fit iron-based superconductors in one correlated regime. Theoretical investigations using multi-orbital models have shown that the values of U distribute in a wide regime.[35] As a result, both the weak-coupling and the strong-coupling models are used in studying iron-based superconductors. So far, the theoretical models can be divided into three kinds: weak-coupling theories, strong-coupling theories, and hybrid theories which are also called local-itinerant theories. The weak-coupling theories, called itinerant theories as well, are focused on the itinerant electrons and regard iron-based superconductors as BCS-like superconductors, with the electron pairing arising from the spin fluctuation exchange. The strong-coupling theories are centered on the local magnetic moments and consider that the superconductivity originates from doping the proximate Mott insulator, which are based on the resonating valence bond (RVB) theories. The hybrid theories combine the above two. They assume that both the itinerant electrons and the local magnetic moments survive and contribute to superconductivity. The itinerant electrons contribute to the Fermi surface, and the local magnetic moments provide the pairing glue.

2. Multi-orbital Hubbard models

The Hubbard model, which was first proposed to describe the magnetism of itinerant electrons in 1963, is the simplest model of interacting particles in a lattice.[36] The Hubbard Hamiltonian is given by

$$H = -t\sum_{i,j,\sigma}\left(c^{\dagger}_{i\sigma}c_{j\sigma}+\text{h.c.}\right)+U\sum_{i}n_{i\uparrow}n_{i\downarrow}, \tag{1}$$

where $c^{\dagger}_{i\sigma}$ $(c_{i\sigma})$ is the creation (annihilation) operator with spin σ, $n_{i\uparrow}$ $(n_{i\downarrow})$ is the number operator for spin up (down) electrons. The first term of the Hamiltonian is the kinetic term describing the hoppings of electrons, and the second item represents the on-site Coulomb interaction.

Although the Hubbard model has a simple form, it can not be solved exactly except for the one-dimensional case. However, we are interested in the situation that the Coulomb interaction is much stronger than the kinetic energy $(U \gg t)$ when studying the cuprate superconductors. In this case, the kinetic term can be treated as a perturbation, and the Hubbard model will transform into the t–J model.

When applying the Hubbard model to iron-based superconductors, we have to consider their multi-orbital nature. There are six electrons in five Fe 3d orbitals. First-principles calculations show that the d_{xz} and d_{yz} orbitals play a key role in the density of states near the Fermi level,[18,19] although we need to include orbitals d_{xy}, $d_{x^2-y^2}$, and $d_{3z^2-r^2}$ too in many cases. In iron-based superconductors, partial 3d electrons are itinerant (e.g., d_{xz} and d_{yz} electrons), the rest of them are mainly localized.[37,38] Theoretically, various multi-orbital models have been proposed to describe the systems, like two-,[39,40] three-,[41,42] four-,[43] and five-orbital Hubbard models.[44,45]

The Hamiltonian for a multi-orbital Hubbard model generally contains two parts

$$H = H_0 + H_{\text{int}}, \tag{2}$$

where H_0 corresponds to the tight-binding part of the Hamiltonian

$$H_0 = \sum_{\boldsymbol{i},\boldsymbol{j}}\sum_{\alpha,\beta}\sum_{\sigma}\left(t^{\alpha,\beta}_{\boldsymbol{i},\boldsymbol{j}}c^{\dagger}_{\boldsymbol{i},\alpha,\sigma}c_{\boldsymbol{j},\beta,\sigma}+\text{h.c.}\right), \tag{3}$$

where $c^{\dagger}_{\boldsymbol{i},\alpha,\sigma}$ creates an electron at site $\boldsymbol{i}$ with spin σ on the α orbital ($\alpha = 1,2,\ldots,5$ stands for the d_{xz}, d_{yz}, d_{xy}, $d_{x^2-y^2}$, and $d_{3z^2-r^2}$ orbitals, respectively). The hopping parameters can be obtained by fitting with experiments and first-principles calculations. The interaction part is

$$\begin{aligned} H_{\text{int}} = {} & U\sum_{\boldsymbol{i},\alpha}n_{\boldsymbol{i},\alpha,\uparrow}n_{\boldsymbol{i},\alpha,\downarrow}+\left(U'-J/2\right)\sum_{\boldsymbol{i}}n_{\boldsymbol{i},\alpha}n_{\boldsymbol{i},\beta} \\ & -2J\sum_{\boldsymbol{i},\alpha<\beta}\boldsymbol{S}_{\boldsymbol{i},\alpha}\cdot\boldsymbol{S}_{\boldsymbol{i},\beta} \\ & +J_{\text{H}}\sum_{\boldsymbol{i},\alpha<\beta}\left(c^{\dagger}_{\boldsymbol{i},\alpha,\uparrow}c^{\dagger}_{\boldsymbol{i},\alpha,\downarrow}c_{\boldsymbol{i},\beta,\downarrow}c_{\boldsymbol{i},\beta,\uparrow}+\text{h.c.}\right), \end{aligned} \tag{4}$$

where $\boldsymbol{S}_{\boldsymbol{i},\alpha}$ $(n_{\boldsymbol{i},\alpha})$ corresponds to the spin (charge density), U, U', J, and J_{H} are the intra-orbital and the inter-orbital Coulomb repulsions, Hund's coupling, and the pairing hopping energy, respectively. Generally, $U' = U - 2J$ and $J_{\text{H}} = J$.[46] Recently, an optical spectroscopy measurement has found that the Hund's coupling greatly affects the correlations.[47]

3. Mean-field approximation

Because of the complexity, it is hard to study the multi-orbital models. A lot of computing methods have been used to deal with them, such as mean-field approximation (MFA), random phase approximation (RPA), fluctuation exchange approximation (FLEX), functional renormalization group (FRG), Gutzwiller variational method, exact diagonalization (ED), dynamical mean-field theory (DMFT), and quantum Monte–Carlo (QMC) method. However, each method has its own limitations. For instance, the exact diagonalization

method can only deal with some small systems, and the well-know sign problem in QMC for Fermi systems is still difficult to be solved.

The mean-field approximation is a useful method to deal with the multi-orbital Hubbard models. We will review this method and use it to study the ground state properties of the two-orbital model in momentum space and real space.

3.1. Momentum space

In the momentum space, it is convenient to deal with the structures which are well defined periodically. The simple standard assumption of the MFA can be written as[42–46]

$$\langle c^{\dagger}_{i,\alpha,\sigma} c_{j,\beta,\sigma'} \rangle = \left[n_\alpha + \frac{\sigma}{2} \cos(\boldsymbol{q}\cdot\boldsymbol{r}_i) m_\alpha \right] \delta_{ij}\delta_{\alpha\beta}\delta_{\sigma\sigma'}, \quad (5)$$

where $\sigma = \pm$ correspond to up and down spins, $\boldsymbol{q}$ is the magnetic order wave vector of the ground state, n_α and m_α describe the charge density and magnetization of orbital α, which can be calculated self-consistently. We can obtain the mean-field interaction Hamiltonian in the momentum space as

$$\begin{aligned} H^{\mathrm{MF}}_{\mathrm{int}} = & \sum_{\boldsymbol{k},\alpha,\sigma} [\varepsilon_\alpha c^{\dagger}_{\boldsymbol{k},\alpha,\sigma} c_{\boldsymbol{k},\alpha,\sigma} \\ & - \eta_{\alpha,\sigma} (c^{\dagger}_{\boldsymbol{k},\alpha,\sigma} c_{\boldsymbol{k}+q,\alpha,\sigma} + \mathrm{h.c.})] + C, \end{aligned} \quad (6)$$

where

$$\begin{aligned} \varepsilon_\alpha &= U n_\alpha + (2U' - J) \sum_{\beta\neq\alpha} n_\beta, \\ \eta_{\alpha,\sigma} &= -\frac{\sigma}{2} \left(U m_\alpha + J \sum_{\beta\neq\alpha} m_\beta \right). \end{aligned}$$

The last term in Eq. (6) is a constant (N is the number of sites)

$$\begin{aligned} C = & -NU \sum_\alpha \left(n_\alpha^2 - \frac{1}{4} m_\alpha^2 \right) - N(2U' - J) \sum_{\alpha\neq\beta} n_\alpha n_\beta \\ & + \frac{NJ}{2} \sum_{\alpha\neq\beta} m_\alpha m_\beta. \end{aligned}$$

The full mean-field Hamiltonian $H^{\mathrm{MF}} = H_0 + H^{\mathrm{MF}}_{\mathrm{int}}$ is quadratic, thus it can be solved with the mean-field parameters n_α and m_α.

3.2. Real space

To investigate the spin, charge, and orbital orderings in real space, it is better to study the real space Hubbard model, especially for the non-periodic structures. It is convenient to use MFA to study the magnetic order and charge density distribution for iron-based superconductors, especially for materials with Fe vacancies, such as $A_x Fe_{2-y} Se_2$ compounds. Similar to the case in the momentum space, the real space Hubbard model can also be studied with the mean-field approximation.[48–50] The first term of the real space Hartree–Fock (HF) approximation to the Coulomb interaction is given by

$$\begin{aligned} H^{\mathrm{HF}}_{\mathrm{int}} = & U \sum_{i,\alpha,\sigma,\sigma'} (-1)^{(1-\delta_{\sigma,\sigma'})} \\ & \times [c^{\dagger}_{i,\alpha,\sigma} c_{i,\alpha,\sigma'} \langle c^{\dagger}_{i,\alpha,-\sigma} c_{i,\alpha,-\sigma'} \rangle \\ & - 1/2 \langle c^{\dagger}_{i,\alpha,\sigma} c_{i,\alpha,\sigma'} \rangle \langle c^{\dagger}_{i,\alpha,-\sigma} c_{i,\alpha,-\sigma'} \rangle]. \end{aligned} \quad (7)$$

The other terms are available in the supplementary of Ref. [48]. In MFA,

$$n_i = \sum_\alpha n_{i,\alpha,\sigma} = \sum_\alpha \langle c^{\dagger}_{i,\alpha,\sigma} c_{i,\alpha,\sigma} \rangle.$$

The other order parameters can be written in a similar way. Numerical calculations are done by iterations for every site in the real space, which means that the expectation values in the HF Hamiltonian are allowed to vary independently from site to site. Results can be obtained self-consistently by minimizing the HF energy. The random initial configurations can be used for each site of the two-dimensional (2D) Fe square lattice, thus there is less biasing towards the correct magnetic order or charge density distribution.[48–50]

4. Results

The two-orbital model is based on the d_{xz} and d_{yz} orbitals, which have been proved to make the dominant contribution to the Fermi surface.[51] It is the simplest multi-orbital model for the iron-based superconductors and can reveal the essential low energy physics of the iron-based superconductors.[39] So it is suitable to use the two-orbital Hubbard model in many cases. The form of this model is the same as that mentioned above. In this section, some results on the real space two-orbital Hubbard model are presented, some of which are in good agreement with experiments.

4.1. Charge and spin stripes in pnictides

We have studied charge stripes in a square lattice by MFA. We find both charge and spin stripes with the periodicity eight in the case of electron doping $\langle n \rangle = 2.33$. The results shown in Fig. 1 are similar to those in Ref. [48]. The charge stripes (Fig. 1(a)) are weaker than the usual Cu-oxides HF stripes, because the charge difference Δn between the maximum $n_{\max}$ and the minimum $n_{\min}$ is smaller than that in cuprates. This result may arise from the fact that the coupling U in pnictides is relatively smaller than that in cuprates. The spin configuration shown in Fig. 1(b) corresponds to the charge stripe state shown in Fig. 1(a). It is found that the spin stripes mainly stay at the locations with the maximum electron density. In the HF minimization, all the expectation values are entangled, therefore it is unclear whether the spin states with domain walls drive the charge stripes or *vice versa*.

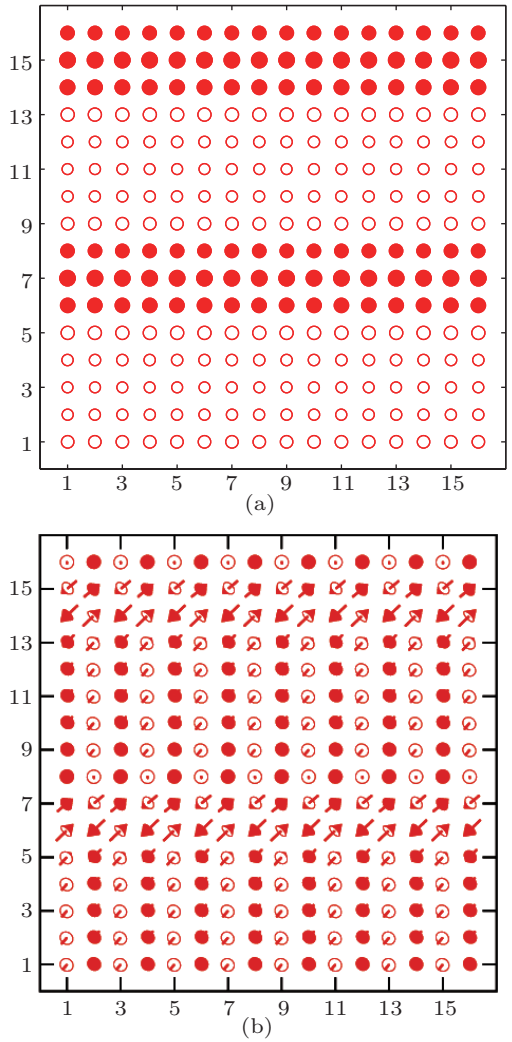


Fig. 1. (a) Charge stripe state of two-orbital model in 16×16 cluster, results are obtained with the HF approximation. The parameters are $t_1 = 0.058$, $t_2 = 0.22$, $t_3 = -0.21$, $t_4 = -0.08$,[52,53] $\langle n \rangle = 2.33$, $U = 0.8$, $J_H/U = 0.25$. The size of the circle is proportional to the charge density. The largest and smallest circles denote $n_{max} = 2.42$ and $n_{min} = 2.27$, respectively. Here, and in other figures, a full (open) circle means that the local density is larger (smaller) than the average. (b) Mean value of the spin in the state shown in panel (a). The positions of the magnetic domain walls are located at the charge stripes, which are inserted in the $(\pi, 0)$ magnetic order background. More details are available in Ref. [48].

4.2. Magnetic orders in *A*–Fe–Se chalcogenides

There are some unique properties in iron-chalcogenide superconductors. For example, ARPES measurements have reported that there are only electron-like pockets at $(\pi, 0)$ and $(0, \pi)$ in their Fermi surfaces.[2,54–56] So the superconductivity in these materials can not be explained by the scattering between the hole- and electron-pockets[57] and the nesting effect.[58,59] The magnetic orders for the alkaline iron selenides are exotic too. For example, at the special composition $K_{0.8}Fe_{1.6}Se_2$ with $\sqrt{5} \times \sqrt{5}$ Fe vacancies, neutron scattering results for this insulating compound reveal an unusual block AFM magnetic order. Theoretical calculations have found the same magnetic results by using the real space five-orbital Hubbard model.[49] In this section, we will show that the results obtained by real space HF approximation of the two-orbital Hubbard model are in good agreement with experiments in different structures of *A*–Fe–Se materials.

4.2.1. Magnetic order for rhombus type iron vacancies

Recently neutron diffraction experiments have revealed the existence of superconductivity in the parent compound of K–Fe–Se, which is an AF semiconductor with a rhombus type iron vacancy order.[60] Its magnetic structure is similar to that of iron pnictides. Superconductivity happens when the AF order is suppressed by electron doping. The novel discovery proves that an AF semiconductor can also induce superconductivity.

Next-next-nearest neighbor (NNNN) hoppings are considered in the real space HF approximation Hubbard model. A lattice with rhombus vacancies on a 16×16 cluster is shown in Fig. 2, with periodic boundary conditions. The hoppings for the nearest neighbor (NN) and the next-nearest neighbor (NNN) are explained in Ref. [39]. Since we focus on the parent magnetic properties, we set $\langle n \rangle = 2.0$. The antiferromagnetic state with rhombus Fe vacancies shown in Fig. 2 is obtained by adjusting the NNNN hoppings t_5, t_6 and Hubbard U. The stripe antiferromagnetic order we obtained is consistent with the results of neutron diffraction experiments.

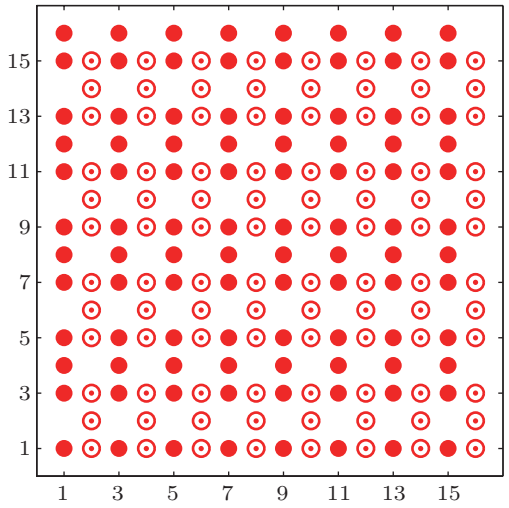


Fig. 2. The parent magnetic state of $K_{0.85}Fe_{1.54}Se_2$ with rhombus Fe vacancies. The parameters are $t_1 = -1.0$, $t_2 = 1.3$, $t_3 = t_4 = -0.85$, $t_5 = -0.27$, $t_6 = 0.16$, $U = 0.8$, $J_H/U = 0.25$.

4.2.2. Effect of Fe vacancies on charge stripes

Recently, many experiments have been carried out to study the compound $A_xFe_{2-y}Se_2$ by transmission electron microscope (TEM),[61] neutron scattering,[8,9] and STM[5,6] because of the discovery of superconductivity with $T_c = 30$ K.[62,63] So far, several different Fe vacancy patterns have been found.[64] Different Fe vacancy patterns can introduce different ground state magnetic structures, such as the block AFM magnetic structure in the $\sqrt{5} \times \sqrt{5}$ Fe vacancy pattern,[8,9,65] A-collinear AFM magnetic structure in

the $\sqrt{2}\times 2\sqrt{2}$ Fe vacancy pattern,[60,66] c-AFM magnetic structure in 2×2 Fe vacancy pattern,[66] and so on. From these measurements, we can see that the Fe vacancies play an important role to the magnetic order and superconductivity. Motivated by these phenomena, we study the charge ordering in a lattice with Fe vacancies.

Figure 3 shows the charge density distributions of different Fe vacancies. For comparison, all the parameters are set to be the same as those in Fig. 1, so it is easy to investigate whether and how the Fe vacancies affect the charge stripes. In Figs. 3(a) and 3(b), only a 3×3 Fe vacancy pattern is introduced on different sites in a 16×16 cluster. We find that stripes can be attracted by Fe vacancies. From our calculations, we find that the Fe vacancies can change the well-ordered stripe phase to the nematic phase. Recently, the electronic nematic phase has been found experimentally in diverse systems, including the cuprate superconductors[67–69] and iron-based superconductors.[70,71] The nematic phase is believed to be a medium to provide the glue for Cooper pairs.

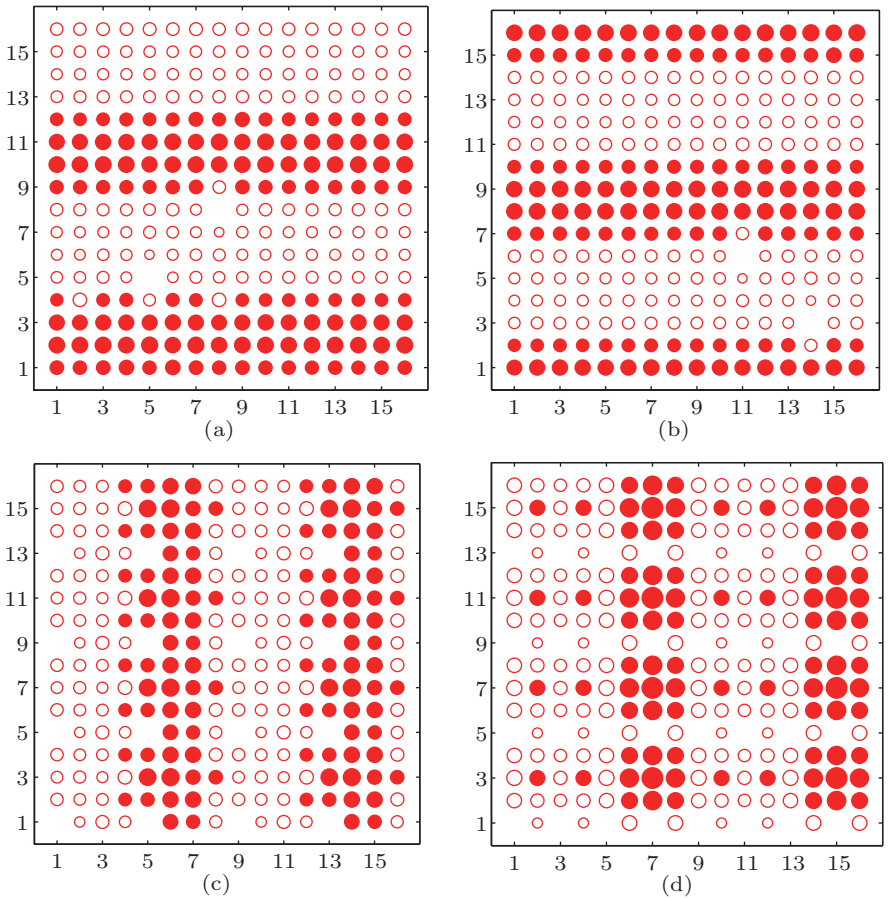


Fig. 3. The ground states of charge density for different Fe vacancy patterns. (a) and (b) Only a 3×3 Fe vacancy pattern exists in different locations, (c) 4×4 type Fe vacancy pattern, and (d) 2×4 type Fe vacancy pattern.

4.2.3. Magnetic order for spin-ladder iron selenides AFe$_2$Se$_3$

The structure of the spin-ladder compounds AFe$_2$Se$_3$ (A = K, Rb, Cs, Ba) is similar to that of iron pnictide superconductors. These compounds contain double chains (ladders) of edge-sharing FeSe$_4$ tetrahedra. It is found that BaFe$_2$Se$_3$ is an insulator. Neutron diffraction measurements[72,73] have shown that the dominant magnetic structure of this 123 material has a block AFM structure, in which four Fe ions form a ferromagnetic cluster (as a unit) and the ferromagnetic blocks couple with each other antiferromagnetically along the ladder direction,[72] as shown in Figs. 4(b) and 4(d). This phenomenon is also reported in K$_{0.8}$Fe$_{1.6}$Se$_2$.[8,9] When BaFe$_2$Se$_3$ is doped with K and changed to Ba$_{1-x}$K$_x$Fe$_2$Se$_3$, the magnetic state transforms from a block antiferromagnet to a stripe antiferromagnet.[73]

To obtain these magnetic states, we use our model in a ladder lattice of size 2×8 with a periodic boundary condition along the ladder direction and an open boundary condition in the rung direction. Numerical results are shown in Figs. 4(a) and 4(b), with hopping amplitudes $t_{1x} = 0.058$, $t_{1y} = 0.116$, $t_{2x} = 0.2196$, $t_{2y} = 0.4329$, $t_3 = -0.20828$, $t_4 = -0.079$. The anisotropy is considered, we assume that the hopping amplitudes along the rung direction are twice as much as those in

the direction along the ladder. The spin stripe magnetic phase appears when the electron density is $\langle n \rangle = 1.6701$ (hole doping). The block magnetic phase appears when $\langle n \rangle = 2.2532$, which corresponds to electron doping. The same results can be obtained by using another set of hopping parameters,[39] as shown in Figs. 4(c) and 4(d). Here $U = 0.8$ and $J_{\rm H}/U = 0.3$ for all these calculations.

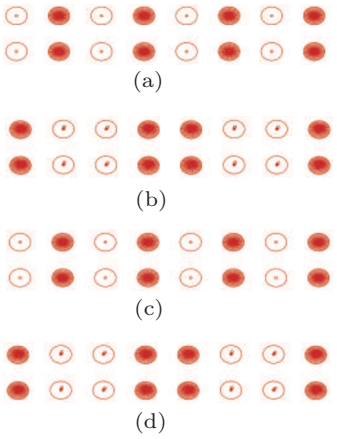


Fig. 4. The magnetic states of spin ladder in $Ba_{1-x}K_xFe_2Se_3$. (a) The result with parameters $t_{1x} = 0.058$, $t_{1y} = 0.116$, $t_{2x} = 0.2196$, $t_{2y} = 0.4329$, $t_3 = -0.20828$, $t_4 = -0.079$, $\langle n \rangle = 1.6701$. (b) The parameters are the same as those in panel (a), but $\langle n \rangle = 2.2532$. (c) The result with parameters $t_1 = -1.0$, $t_2 = 1.3$, $t_3 = t_4 = -0.85$, $\langle n \rangle = 1.16$. (d) The parameters are the same as those in panel (c), but $\langle n \rangle = 2.65$.

4.3. Orbital ordering

Laser angle resolved photoemission spectroscopy (laser-ARPES) experiments have shown that the observed cut of the Fermi surface in the AF state is dominantly composed of the Fe $3d_{xz}$ orbital.[74,75] Theoretical calculations from the three- and five-orbital models have the same conclusion that the states near the Fermi surface have more d_{xz} characters than d_{yz}.[76,77]

Orbital ordering or anisotropy, which always coexists with spin ordering, is considered as the origin of the structural distortion. The d_{xz} and d_{yz} orbitals are the only two 3d orbitals breaking the lattice C_4 rotational symmetry locally. For the systems favored by the d_{xz} orbital, the inequivalence between the d_{xz} and d_{yz} orbitals breaks the C_4 rotational symmetry and induces a structural distortion.

To investigate the orbital ordering, different numerical methods have been used, including the MFA. For example, a very weak orbital ordering has been found in the two-orbital model in the half-filled case.[78]

5. Summary

In this paper, we have reviewed some spin, charge, and orbital orderings in iron-based superconductors, as well as the multi-orbital Hubbard models. We have shown some results of the multi-orbital models to illustrate the properties. They are in agreement with experiments. Meanwhile the mean-field approximation has been introduced.

On certain dopings, spin and charge stripes appear and are connected with the orbital ordering or anisotropy. For instance, the $(\pi, 0)$-AF order gives rise to the inequality of orbitals so the d_{xz} orbitals may be more populated than d_{yz}.[76] This can be the origin of the orbital ordering. On the other hand, the orbital ordering affects the spin and charge orderings. Meanwhile the nematic order has been found in the superconducting phase, which is thought as a medium to provide the glue for Cooper pairs. Thus the disorder may be important for the macroscopic superconductivity in iron-based superconductors and cuprate superconductors. It is reasonable to believe that the spin, charge, orbital orderings and the superconducting order can couple to each other. These orderings may provide the medium for superconductivity. However, these orderings may also be resulted from the superconductivity.

References

[1] Kamihara Y, Watanabe T, Hirano M and Hosono H 2008 *J. Am. Chem. Soc.* **130** 3296
[2] Zhang Y, Yang L X, Xu M, Ye Z R, Chen F, He C, Xu H C, Jiang J, Xie B P, Ying J J, Wang X F, Chen X H, Hu J P, Matsunami M, Kimura S and Feng D L 2011 *Nat. Mater.* **10** 273
[3] Ding H, Qian T and Wang X P 2011 *Physics* **40** 523 (in Chinese)
[4] Hoffman J E 2011 *Rep. Prog. Phys.* **74** 124513
[5] Li W, Ding H, Deng P, Chang K, Song C L, He K, Wang L L, Ma X C, Hu J P, Chen X and Xue Q K 2012 *Nat. Phys.* **8** 126
[6] Cai P, Ye C, Ruan W, Zhou X D, Wang A F, Zhang M, Chen X H and Wang Y Y 2012 *Phys. Rev. B* **85** 094512
[7] Zhao J, Adroja D T, Yao D X, Bewley R, Li S L, Wang X F, Wu G, Chen X H, Hu J P and Dai P C 2009 *Nat. Phys.* **5** 555
[8] Bao W, Huang Q Z, Chen G F, Green M A, Wang D M, He J B and Qiu Y M 2011 *Chin. Phys. Lett.* **28** 086104
[9] Ye F, Chi S, Bao W, Wang X F, Ying J J, Chen X H, Wang H D, Dong C H and Fang M 2011 *Phys. Rev. Lett.* **107** 137003
[10] Zhou K J, Huang Y B, Monney C, Dai X, Strocov V N, Wang N L, Chen Z G, Zhang C L, Dai P C, Patthey L, van den Brink J, Ding H and Schmitt T 2013 *Nat. Commun.* **4** 1470
[11] Hasan M Z, Isaacs E D, Shen Z X, Miller L L, Tsutsui K, Tohyama T and Maekawa S 2000 *Science* **288** 1811
[12] Zhang X D, Wu W, Zheng P, Wang N L and Luo J L 2012 *Chin. Phys. B* **21** 017402
[13] Haule K, Shim J H and Kotliar G 2008 *Phys. Rev. Lett.* **100** 226402
[14] Liu C, Samolyuk G D, Lee Y, Ni N, Kondo T, Santander-Syro A F, Bud'ko S L, McChesney J L, Rotenberg E, Valla T, Fedorov A V, Canfield P C, Harmon B N and Kaminski A 2008 *Phys. Rev. Lett.* **101** 177005
[15] Borisenko S V, Zabolotnyy V B, Evtushinsky D V, Kim T K, Morozov I V, Yaresko A N, Kordyuk A A, Behr G, Vasiliev A, Follath R and Büchner B 2010 *Phys. Rev. Lett.* **105** 067002
[16] Sefat A S, Jin R, McGuire M A, Sales B C, Singh D J and Mandrus D 2008 *Phys. Rev. Lett.* **101** 117004
[17] Rotter M, Tegel M and Johrendt D 2008 *Phys. Rev. Lett.* **101** 177006
[18] Mazin I I, Singh D J, Johannes M D and Du M H 2008 *Phys. Rev. Lett.* **101** 057003
[19] Vildosola V, Pourovskii L, Arita R, Biermann S and Georges A 2008 *Phys. Rev. B* **78** 064518
[20] Seo K, Bernevig B A and Hu J 2008 *Phys. Rev. Lett.* **101** 206404
[21] Kuroki1 K, Onari S, Arita R, Usui1 H, Tanaka Y, Kontani H and Aoki H 2008 *Phys. Rev. Lett.* **101** 087004
[22] Wang F and Lee D H 2011 *Science* **332** 200
[23] Yildirim T 2008 *Phys. Rev. Lett.* **101** 057010

[24] Ma F, Lu Z Y and Xiang T 2008 *Phys. Rev. B* **78** 224517

[25] Si Q and Abrahams E 2008 *Phys. Rev. Lett.* **101** 076401

[26] Yao D X and Carlson E W 2008 *Phys. Rev. B* **78** 052507

[27] Yao D X and Carlson E W 2010 *Front. Phys. China* **5** 161

[28] Wang M, Chen F, Yao D X, Tan G T, Harriger L W, Song Y, Netherton T, Zhang C, Wang M, Stone M B, Tian W, Hu J and Dai P 2011 *Nat. Commun.* **2** 580

[29] Zhao J, Yao D X, Li S, Hong T, Chen Y, Chang S, II R W, Lynn J W, Mook H A, Chen G F, Luo J L, Wang N L, Carlson E W, Hu J and Dai P 2008 *Phys. Rev. Lett.* **101** 167203

[30] Hu J and Hao N 2012 *Phys. Rev. X* **2** 021009

[31] Qazilbash M M, Hamlin J J, Baumbach R E, Zhang L, Singh D J, Maple M B and Basov D N 2009 *Nat. Phys.* **5** 647

[32] Dai J H, Si Q M, Zhu J X and Abrahams E 2009 *Proc. Natl. Acad. Sci. USA* **11** 4118

[33] Yao D X 2011 *Front. Phys. China* **6** 344

[34] Guidry M, Sun Y and Wu C L 2009 *Front. Phys. China* **4** 433

[35] Dai P, Hu J and Dagotto E 2012 *Nat. Phys.* **8** 709

[36] Hubbard J 1963 *Proc. Roy. Soc. A* **276** 238

[37] Kou S P, Li T and Weng Z Y 2009 *Europhys. Lett.* **88** 17010

[38] Yin W G, Lee C C and Ku W 2010 *Phys. Rev. Lett.* **105** 107004

[39] Raghu S, Qi X L, Liu C X, Scalapino D J and Zhang S C 2008 *Phys. Rev. B* **77** 220503

[40] Ran Y, Wang F, Zhai H, Vishwanath A and Lee D H 2009 *Phys. Rev. B* **79** 014505

[41] Lee P A and Wen X G 2008 *Phys. Rev. B* **78** 144517

[42] Daghofer M, Nicholson A, Moreo A and Dagotto E 2010 *Phys. Rev. B* **81** 014511

[43] Yu R, Trinh R T, Moreo A, Daghofer M, Riera J A, Haas S and Dagotto E 2009 *Phys. Rev. B* **79** 104510

[44] Graser S, Maier T A, Hirschfeld P J and Scalapino D J 2009 *New J. Phys.* **11** 025016

[45] Luo Q L, Martins G, Yao D X, Daghofer M, Yu R, Moreo A and Dagotto E 2010 *Phys. Rev. B* **82** 104508

[46] Dagotto E, Hotta T and Moreo A 2001 *Phys. Rep.* **344** 1

[47] Yuan R H, Kong W D, Yan L, Ding H and Wang N L 2013 *Phys. Rev. B* **87** 144517

[48] Luo Q L, Yao D X, Moreo A and Dagotto E 2011 *Phys. Rev. B* **83** 174513

[49] Luo Q L, Nicholson A, Riera J, Yao D X, Moreo A and Dagotto E 2011 *Phys. Rev. B* **84** 140506

[50] Luo Q L, Nicholson A, Rincon J, Liang S H, Riera J, Alvarez G, Wang L M, Ku W, Samolyuk G D, Moreo A and Dagotto E 2013 *Phys. Rev. B* **87** 024404

[51] Boeri L, Dolgov O V and Golubov A A 2008 *Phys. Rev. Lett.* **101** 026403

[52] Daghofer M, Moreo A, Riera J A, Arrigoni E, Scalapino D J and Dagotto E 2008 *Phys. Rev. Lett.* **101** 237004

[53] Moreo A, Daghofer M, Riera J A and Dagotto E 2009 *Phys. Rev. B* **79** 134502

[54] Mou D X, Liu S Y, Jia X W, He J F, Peng Y Y, Zhao L, Yu L, Liu G D, He S L, Dong X L, Zhang J, Wang X D, Dong C H, Fang M H, Wang X Y, Peng Q J, Wang Z M, Zhang S J, Yang F, Xu Z Y, Chen C T and Zhou X J 2011 *Phys. Rev. Lett.* **106** 107001

[55] Qian T, Wang X P, Jin W C, Zhang P, Richard P, Xu G, Dai X, Fang Z, Guo J G, Chen X L and Ding H 2011 *Phys. Rev. Lett.* **106** 187001

[56] Shermadini Z, Krzton-Maziopa A, Bendele M, Khasanov R, Luetkens H, Conder K, Pomjakushina E, Weyeneth S, Pomjakushin V, Bossen O and Amato A 2011 *Phys. Rev. Lett.* **106** 117602

[57] Chen F, Xu M, Ge Q Q, Zhang Y, Ye Z R, Yang L X, Jiang J, Xie B P, Che R C, Zhang M, Wang A F, Chen X H, Shen D W, Hu J P and Feng D L 2011 *Phys. Rev. X* **1** 021020

[58] Wang X P, Qian T, Richard P, Zhang P, Dong J, Wang H D, Dong C H, Fang M H and Ding H 2011 *Europhys. Lett.* **93** 57001

[59] Wang K, Lei H and Petrovic C 2011 *Phys. Rev. B* **83** 174503

[60] Zhao J, Cao H B, Bourret-Courchesne E, Lee D H and Birgeneau R J 2012 *Phys. Rev. Lett.* **109** 267003

[61] Wang Z, Song Y J, Shi H L, Wang Z W, Chen Z, Tian H F, Chen G F, Guo J G, Yang H X and Li J Q 2011 *Phys. Rev. B* **84** 140505

[62] Guo J G, Jin S F, Wang G, Wang S C, Zhu K X, Zhou T T, He M and Chen X L 2010 *Phys. Rev. B* **82** 180520

[63] Krzton-Maziopa A, Shermadini Z, Pomjakushina E, Pomjakushin V, Bendele M, Amato A, Khasanov R, Luetkens H and Conder K 2011 *J. Phys.: Condens. Matter* **23** 052203

[64] Mou D X, Zhao L and Zhou X J 2011 *Front. Phys. China* **6** 410

[65] Cao C and Dai J 2011 *Phys. Rev. Lett.* **107** 056401

[66] Yan X W, Gao M, Lu Z Y and Xiang T 2011 *Phys. Rev. Lett.* **106** 087005

[67] Ando Y, Segawa K, Komiya S and Lavrov A N 2002 *Phys. Rev. Lett.* **88** 137005

[68] Hinkov V, Haug D, Fauqué B, Bourges P, Sidis Y, Ivanov A, Bernhard C, Lin C T and Keimer B 2008 *Science* **319** 597

[69] Howald C, Eisaki H, Kaneko N and Kapitulnik A 2003 *Proc. Natl. Acad. Sci. USA* **100** 9705

[70] Chuang T M, Allan M P, Lee J, Xie Y, Ni N, Bud'ko S L, Boebinger G S, Canfield P S and Davis J C 2010 *Science* **327** 181

[71] Fradkin E and Kivelson S A 2010 *Science* **327** 155

[72] Nambu Y, Ohgushi K, Suzuki S, Du F, Avdeev M, Uwatoko Y, Munakata K, Fukazawa H, Chi S X, Ueda Y and Sato T J 2012 *Phys. Rev. B* **85** 064413

[73] Caron J M, Neilson J R, Miller D C, Arpino K, Llobet A and McQueen T M 2012 *Phys. Rev. B* **85** 180405

[74] Shimojima T, Ishizaka K, Ishida Y, Katayama N, Ohgushi K, Kiss T, Okawa M, Togashi T, Wang X Y, Chen C T, Watanabe S, Kadota R, Oguchi T, Chainani A and Shin S 2010 *Phys. Rev. Lett.* **104** 057002

[75] Yi M, Lu D, Chu J H, Analytis J G, Sorini A P, Kemper A F, Moritz B, Mo S K, Moore R G, Hashimoto M, Lee W S, Hussain Z, Devereaux T P, Fisher I R and Shen Z X 2010 *Proc. Natl. Acad. Sci. USA* **108** 6878

[76] Daghofer M, Luo Q L, Yu R, Yao D X, Moreo A and Dagotto E 2010 *Phys. Rev. B* **81** 180514

[77] Su Y and Li T 2013 arXiv: 1303.7302

[78] Kubo K and Thalmeier P 2009 *J. Phys. Soc. Jpn.* **78** 083704